Identification of sdBV star pulsed modes

Radosław Kluczewski[1]

Faculty of Physics, Astronomy and Applied Computer Science of the Jagiellonian University
e-mail: radek.info.klucz@gmail.com

14 lipca 2022

STRESZCZENIE

Objective. Obtaining a list of pulsed frequencies of an sdBV star with quantum numbers l, n, m.
Method. The use of shared programs for calculating the Fourier transform and the python language for data processing.
Results. List of pulsed frequencies with period, amplitude and quantum numbers.

1. Theoretical basics

Pulsating stars are variable stars that change their brightness, size and shape periodically. Periodicity is related to the occurrence of a partial ionization layer in the outer regions of the star, which under certain conditions destabilizes the star by first contracting it and then expanding around the equilibrium position. Based on the observation of the frequency spectrum of the pulsations, astroseismology, i.e. the field of astrophysics that studies these pulsations and vibrations, is able to obtain information about the interior of the studied star.

Vibrations of the star gas occur in three dimensions, so theoretical description uses quantum integers **n**, **l**, **m**. The number **n** describes the radial order of magnitude of the mode, that is, it contains the number of nodal surfaces inside the star. These surfaces do not take part in the movement, only separating the layers in which the gas moves in different directions. The angular degree of the **l** mode gives information about the number of nodal planes on the star's surface, while the azimuth **m** degree gives information about the lines passing through the poles of the pulsating star. Node lines divide the star into regions where the physical conditions change as a result of pulsations in opposite phases (for example, changes in brightness).

When $|m| \leq l$ then for a given module m describes the side lobe of the module located on the left and right sides (symmetrically) of the Fourier transform with respect to the central lobe. When a pulsating star is spherical and the slow rotation approximation is used, the multiplet mode frequencies are proportional to the star's rotation frequency. Thus, on the basis of the intervals between successive frequencies of the multiplet, the rotation of the star can be determined.

2. Performing the exercise

The sdB93.data file was used to perform the exercise, which contains data about the brightness curve of a pulsed star. Additionally, sources [1] and [2] were used during data compilation.

2.1. Calculation of the Fourier transform from the selected brightness curve

In order to perform the calculations, the *jkft50* program, which calculates the Fourier transform, was used. The resulting file, after running the program, is the Fourierive amplitude spectrum, which includes frequency columns in [c/d] and frequency amplitudes in [ppt] units.

2.2. Calculation of the noise level of the amplitude spectrum

Using the *ftnoise* program, the detection level ranging from 0 to 50 cycles per day was calculated, the value of which was: 0.037. The above result corresponds to a noise detection level of $4 \cdot \sigma$, where σ is the average noise floor of the Fourier transform. This result is marked in the picture 1.

2.3. Spectrum signals identification

The *scipy* module and the *find peaks* function were used to identify spectrum signals that exceed the noise level set. Additionally, a spectral window was generated by means of which the signals constituting artifacts of the Fourier transform were eliminated. The identified signals without artifacts are summarized in Table 1, with frequency and period recorded for each identified "peak".

The spectral windows are presented in the picture 2 and the picture 3. To draw the spectral window, it was necessary to prepare a sinusoid for points with the same time distribution as for the sdB93 data, which will be used to identify multiplets and triplets (m numbers for a given l).Next, the Fourier transform was calculated for the generated sine wave, which was compared with the signals with the highest amplitudes, close to which the possible components of the multiplets also have high amplitudes. From the spectral window, it is possible to determine which signals are artifacts. After eliminating the mentioned artifacts, we are able to correctly identify the true components of multilipets (if they exist).

2.4. Converting the $f_i[c/d]$ frequency list to $P_i[s]$ periods

The signals found along with the entire sdB93 data range were converted from frequency in units of cycles per day to periods in seconds. The conversion formula is presented below:

$$\frac{86400}{i},$$

where the number 86400 is a day expressed in seconds, and i is the frequency from the data transform. The signals in the periods are listed in Table 1 and in fig.4, which shows the amplitude

spectrum of the Fourier transform as a function of the period in seconds. Additionally, in the picture **??** the so-called mod ladder is presented, i.e. the fourier transform amplitude spectrum plotted with the equidistant dots of the mods l_1 (272.62 seconds, green color), l_2 (151.92 seconds, blue color)) and l_3 (78.23 seconds, black). The ladder was developed with the help of the identified modes shown in fig.2 and fig.3. From the figures cited, the central frequencies of the peaks were read, which were the starting points for the equidistant dots. Then, successive dots were plotted for a given number l = 1 and l = 2 with distances equal to 272.62 seconds and 151.92 seconds, respectively, on both sides of the center mode frequency, until the entire range of the Fourier transform is filled.

2.5. Finding the distance Pi_{l_1}, Pi_{l_2} for the l_1 and l_2 series

For pulsating stars, the sdBV in the space of the pulsation mode periods for a given l are approximately equal spacing. The distance between the n and $n + 1$ modes is approximately 245 seconds for $l = 1$ and 140 seconds for $l = 2$. For the modes defined in this way, the data was divided by assigning them the values of l_1 and l_2 in advance in order to obtain transparent histograms. Initially, the data was divided into parts with periods $T < 4500$ and $T > 4500$, where a distance of 245 seconds was expected for the first range, and 140 seconds for the second. This solution did not bring the expected results because it eliminated a significant part of the distance between the signals. Ultimately, it was decided not to divide the data into two parts, but to calculate the distance for the entire data range without pre-assignment. Then, using the python language, the *math* module and the *dist* function, the distances to be searched were calculated. The formula for calculating the distances is presented below:

$$d(x_i, x_j) = |(x_i - x_j)|, \tag{1}$$

where x_i and x_j are respectively x coordinates of the identified signals expressed in periods. fig.6 presents a histogram of the distribution of the occurrence of a given distance from the distance between the signals. As you can see, the plotted distance histogram for the data has successive mods in the distance $n \cdot \Pi$, where Π is the distance for a given l.

2.6. Identification of mods

To identify the modes, a histogram was used for the entire data with a bar width of 12 seconds, fig.6, to which Gaussian functions were fitted, where the fields under the graph were normalized to one. The intervals for fitting Gaussian functions are respectively for Fig.**??** with a bar width of 3 seconds and for fig.8 with a bar width of 4 seconds, intervals of 120 - 190 seconds and 240 - 300 seconds. The fit parameters are:

- $\mu_{l_1} = 272.62$,
- $\sigma_{l_1} = 5.82$,
- $\mu_{l_2} = 151.92$,
- $\sigma_{l_2} = 8.01$.

For the matching parameters thus obtained, the modes of individual signals were then identified, where the identification of a given mode was based on the following histogram width ranges:

$$(\mu_2 - \sigma_2, \mu_2 + \sigma_2).$$

If modes giving such a space were found in a given interval of intervals, then the mod was identified as l_1 (the first range) or l_2 (for the second range).

Additionally, in the histogram for the totality of the data in fig.6 one can see a small maximum corresponding to the distance between the periods of approximately 80 seconds, which may correspond to the intervals between the periods for l = 3. For these distances, the Gaussian function was also fitted fig.9, where the width of the histogram bars is 3 seconds with the following interval 70 - 90 seconds and parameters:

- $\mu_{l_3} = 78.23$,
- $\sigma_{l_3} = 1.51$,

Then the modes were identified in the same way as above. The results of all identified modes are presented in Table 1.

The justification for the distance of approximately 80 seconds results from the following formula taken from publication [3], where the distance between the modes with l = 3 is described as follows:

$$DP(l = 3) = \frac{1}{2} \cdot DP(l = 1). \tag{2}$$

In the above formula, DP (l = 1) is the distance between modes for l = 1. So for l = 1 of approximately 150 seconds we are able to assign a peak l = 3 of approximately 80 seconds.

The number n describing the radial row has also been identified. This number was assigned to $l = 1$ and $l = 2$ starting at $n = 1$. When the identified signals expressed in periods are 272.62 seconds and 151.92 seconds apart, they are assigned relative values of n, respectively, where for the next equidistant signal the number of the radial order will be $n = n_{current} + 1$. The missing equidistant mod in the sequence increases n by 1, so there are also gaps not assigned a number of n between the periods. Table 1 shows the identified radial order number n with the expected gaps.

2.7. Visual identification of multiplets

In order to confirm the identification from the so-called mode ladder fig.5 visual identification of the multiplets was made. Thus, for the modes with the highest amplitudes, multiplet components were found, where $|m|$ *leql*. Examples of identifications are presented in the picture 2 and in the picture 3. As can be seen in the first figure, we can see symmetrical signals with respect to the centered peak for $1 = 2$, which protrude above the detection level, and the drawn sine wave. These signals were respectively identified as $m = -2, -1, +1, +2$. Similarly, visual identification was carried out in the second figure, which shows the central signal for l = 1 with the detection level plotted and the fitted sinusoid. Identified symmetrical signals projecting above the detection level and sine waves are described by the following numbers $m = -1, +1$. All identified m numbers are presented in Table 1.

2.8. Designation Confirmation Π

In order to confirm the determination of Π, the Fourier transform was calculated from the amplitude spectrum but converted to period. Before performing the calculations, using the *jkft50* program, the range of the Fourier transform was limited to 20,000 seconds and sorted in ascending order with respect to the period column. For the data prepared in this way, the transform was

calculated, the results of which are presented in fig.10. By comparing the graph with the obtained maxima of the histograms in frequencies, which were marked in the above-mentioned figure, respectively $\sigma_1 = 1/151.92$ and $\sigma_2 = 1/272.62$, you can try to confirm the correctness of determining the distance between the mode series periods for a given l, which should be seen in the Fourier transform from the period-converted amplitude spectrum.

3. Discussion of the results

By using the python programming language, it was possible to identify the l_1, l_2 and l_3 modes. It is also worth noting the number of peaks identified, the number being 130. This is the expected number of peaks for sdBV stars. The larger number was due to the use of a programming language function that counts all signals and artifacts above a predetermined detection level. Most of the artifacts were visually eliminated through the use of a spectral window. Attempts were also made to eliminate artifacts by including the *prominence* filter in the *find peaks* function, but no significant improvement was noticed for the histogram. The use of the filter cut the distance which resulted in fitting the Gaussian function for a small number of counts. As a consequence, it also influenced the correct identification of modes, where for the mentioned distance there were practically no identifiable numbers $l = 1$. Finally, it was decided to fit the Gaussian function for signals -80, - 155, - 270 for all data without applying a filter. The identification of the number of the radial order n confirms the assumption that there is a gap that does not have the assigned value of the number n. The visual identification of the number m confirmed the existence of multiplets. On the other hand, the maxima of the histograms for individual signals equal respectively: $\sigma_1 = 1/151.92$ and $\sigma_2 = 1/272.62$ coincide with the graph confirming the designation of Π, so the identification of the mods was correctly made. By using the python programming language the l_1, l_2 and l_3 mods were identified. It is also worth noting the number of peaks identified, the number being 130. This is the expected number of peaks for sdBV stars. The larger number was due to the use of a programming language function that counts all signals and artifacts above a predetermined detection level. Most of the artifacts were visually eliminated through the use of a spectral window. Attempts were also made to eliminate artifacts by including the *prominence* filter in the *find peaks* function, but no significant improvement was noticed for the histogram. The use of the filter cut the distance which resulted in fitting the Gaussian function for a small number of counts. As a consequence, it also influenced the correct identification of modes, where for the mentioned distance there were practically no identifiable numbers $l = 1$. Finally, it was decided to fit the Gaussian function for signals -80, - 155, - 270 for all data without applying a filter. The identification of the number of the radial order n confirms the assumption that there is a gap that does not have the assigned value of the number n. The visual identification of the number m confirmed the existence of multiplets. On the other hand, the maxima of the histograms for individual signals equal to $\sigma_1 = 1/151.92$ and $\sigma_2 = 1/272.62$, respectively, coincide with the graph confirming the designation of Π, so the identification of the mods was correctly made.

4. Reference

1. Jerzy Krzesinski, 2015, A&A 581, A7, 7
2. Radosław Smolec, Asterosejsmologia – probing the interior of stars, Astronomical Center for them. Nicholas Copernicus, Warsaw
3. J. Krzesiński, A. Blokesz, A.S. Baran, S. Bachulski, 2014, AA, 64, 151–165

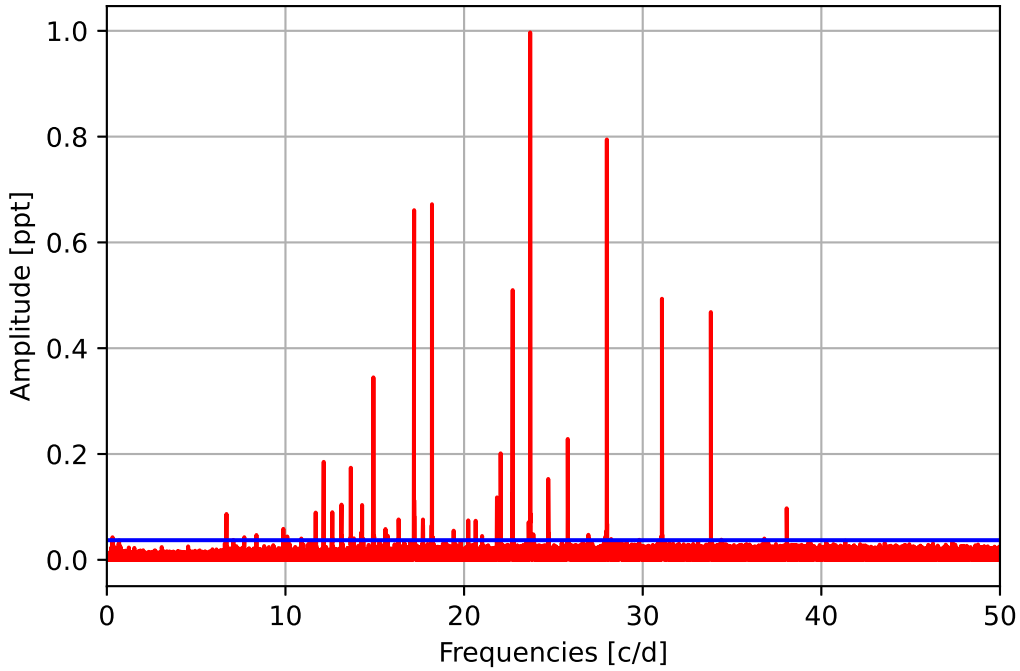

Rysunek 1: The amplitude spectrum of a pulsating star in red with the detection level in blue.

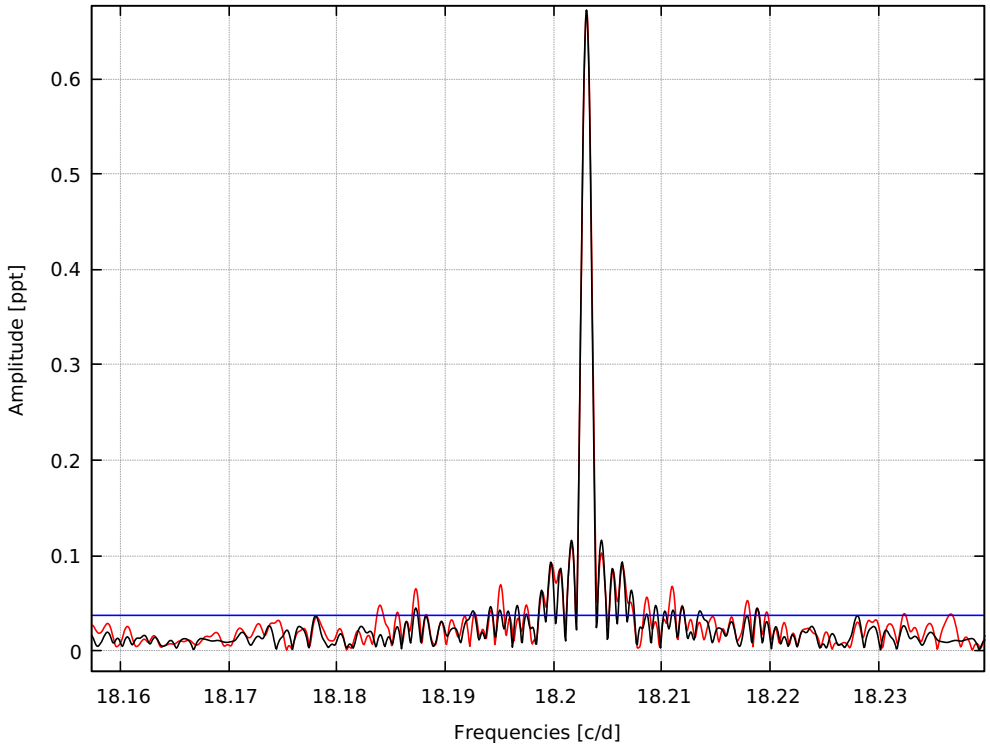

Rysunek 2: Spectral window superimposed on the pulsed mode with the frequency 18.203054 [c/d]. Apart from the main frequency, there are also visible weak multiplet signals, two on each side of the frequency 18.203054 [c / d] (ie 18.187281, 18.195129 and on the other side of the central peak 18.210979, 18.217905). Thus, the mod can be identified as $l = 2$, where red is the amplitude spectrum of the data, black is the generated sinusoidal amplitude spectrum, and blue is the detection level of the amplitude spectrum.

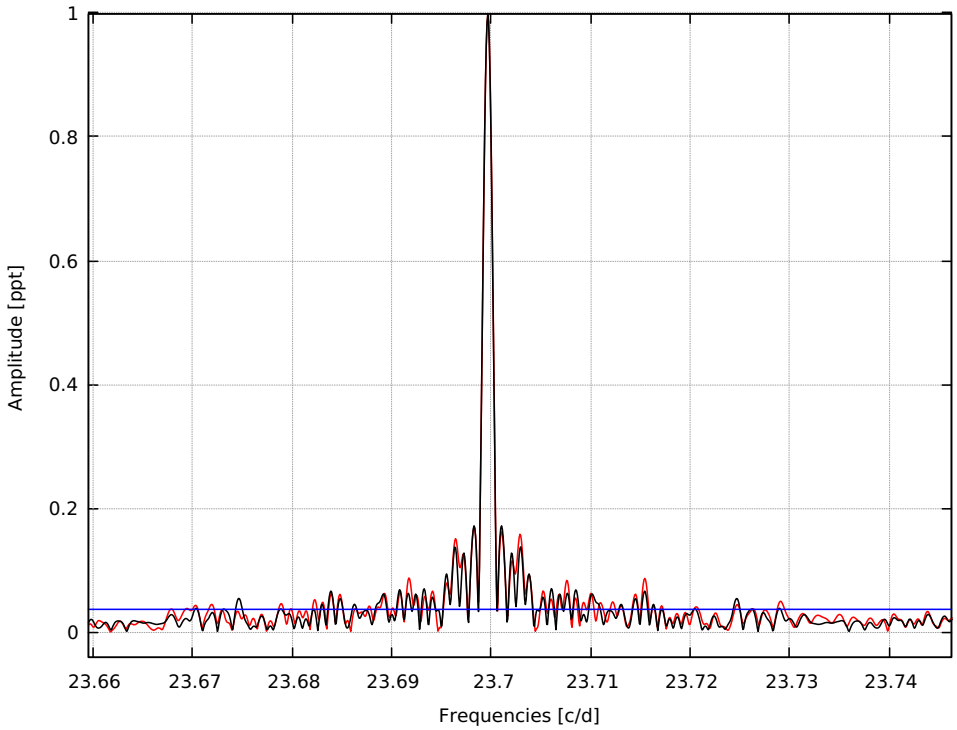

Rysunek 3: Spectral window superimposed on the pulse mode with the frequency 23.69969 [c / d]. Apart from the main frequency, there are also visible weak multlet signals, two on each side of the 23.69969 [c / d] frequency (ie 23.691763 and on the other side of the central peak 23.707615). Thus, the mod can be identified as $l = 1$, where red is the amplitude spectrum of the data, black is the generated sinusoidal amplitude spectrum, and blue is the detection level of the amplitude spectrum.

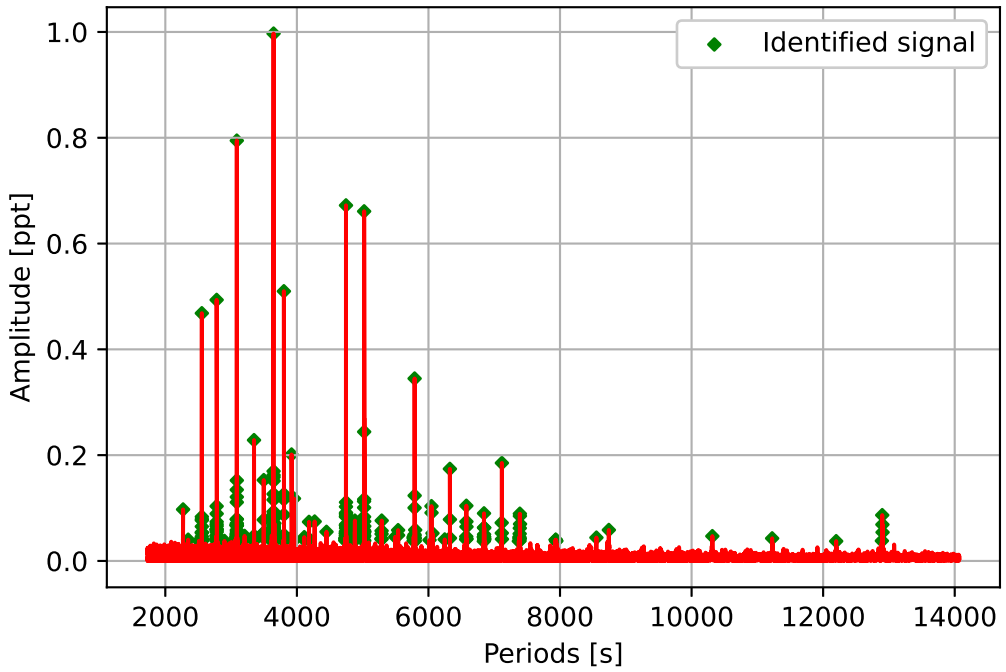

Rysunek 4: Converted (see 2.4) spectrum of the Fourier transform with plotted signals.

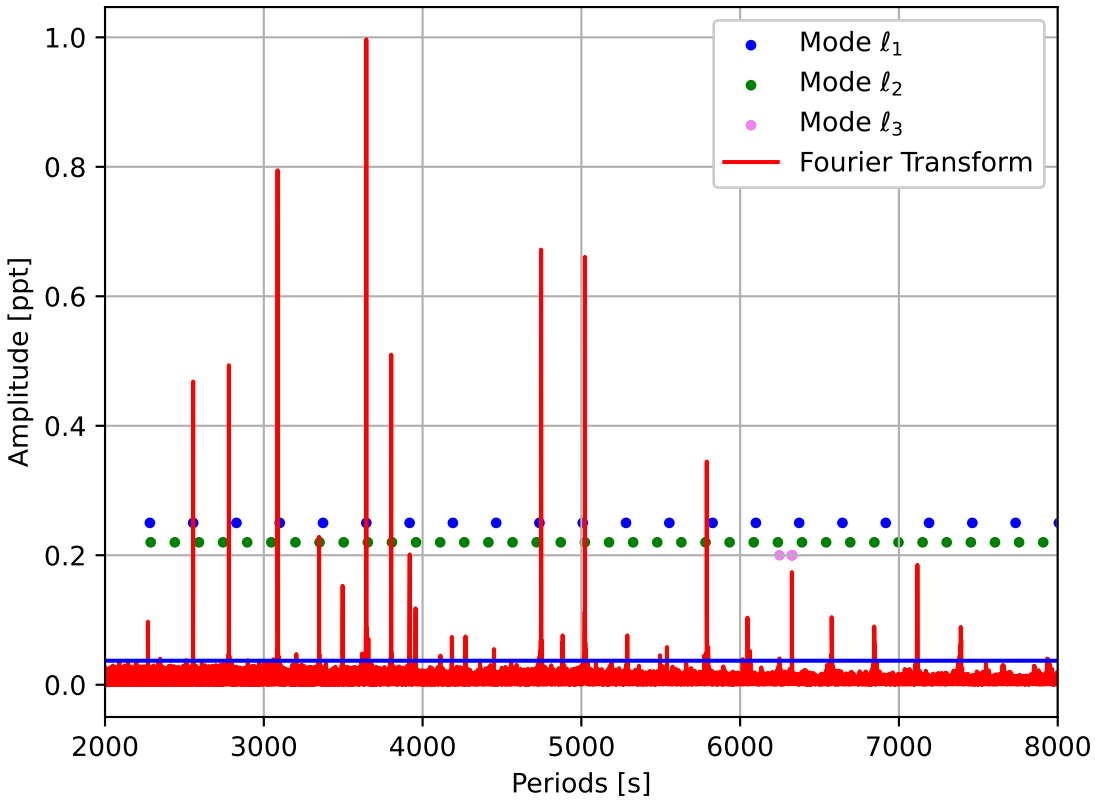

Rysunek 5: Converted amplitude spectrum with plotted signal modes.

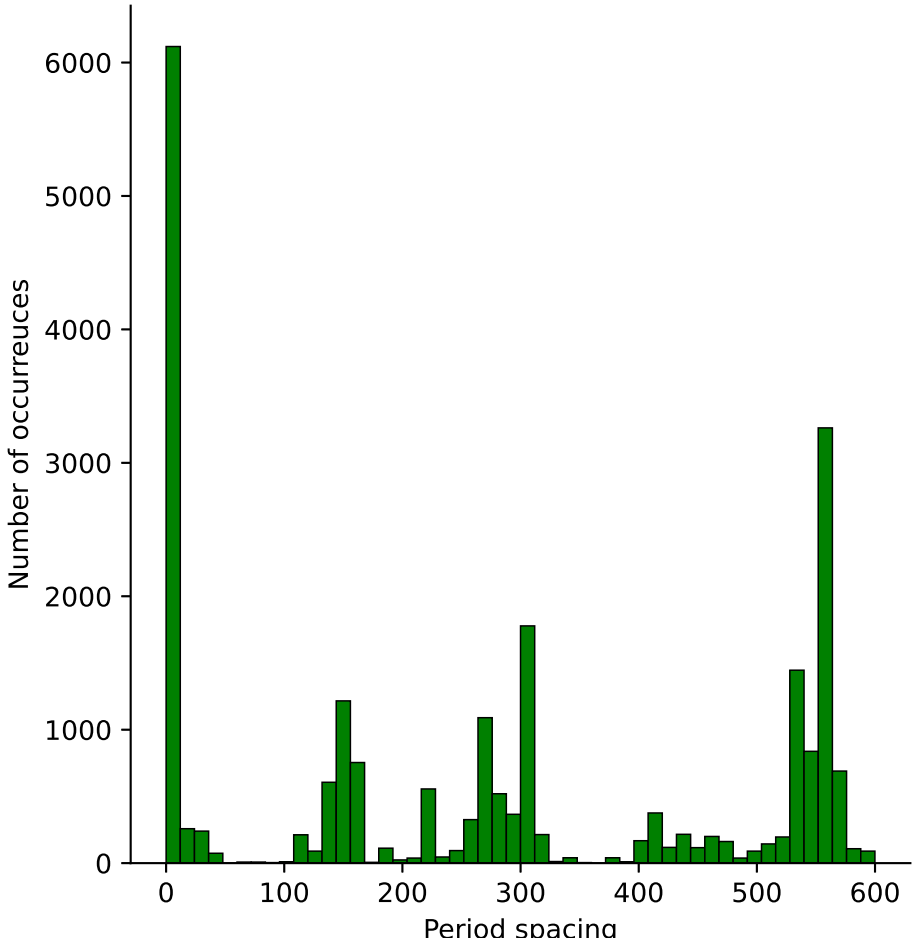

Rysunek 6: A histogram that shows the distance distribution for the data, where the bars are 12 seconds wide.

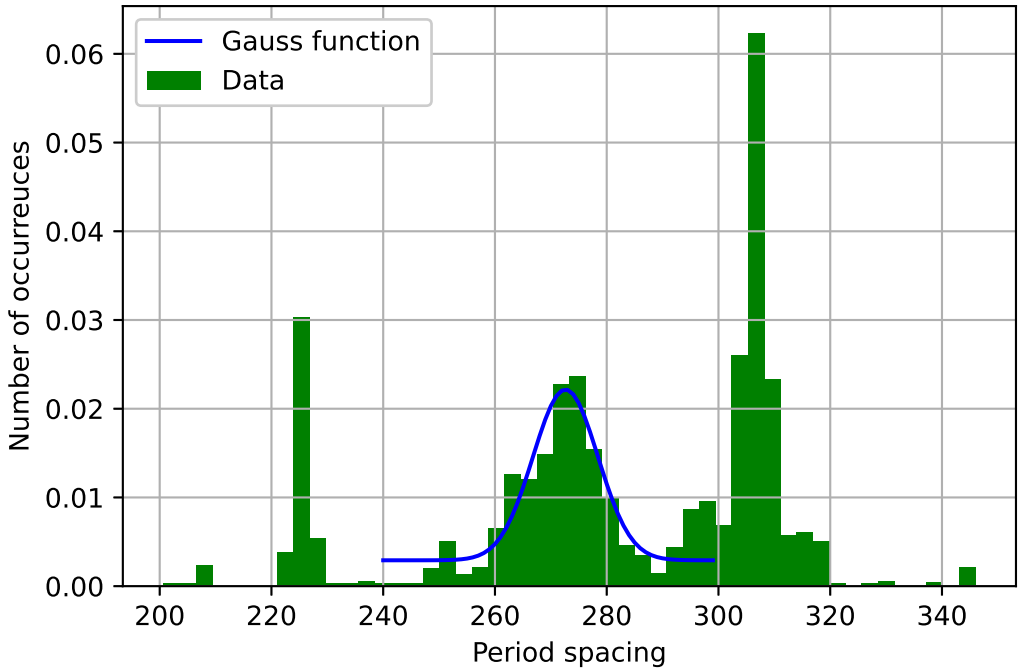

Rysunek 7: Histogram showing the distance distribution for $l = 1$ with fitted Gaussian function in the range 240 to 300 seconds, where the bars are 3 seconds wide.

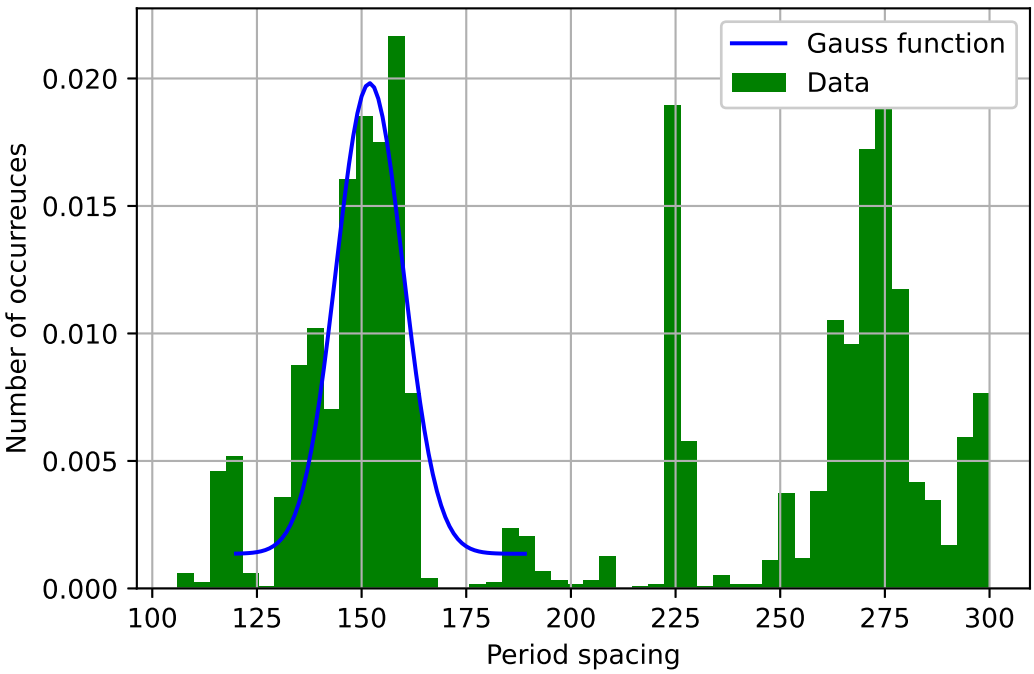

Rysunek 8: Histogram showing the distance distribution for $l = 2$ with fitted Gaussian function in the range from 120 to 190 seconds, where the width of the bars is 4 seconds.

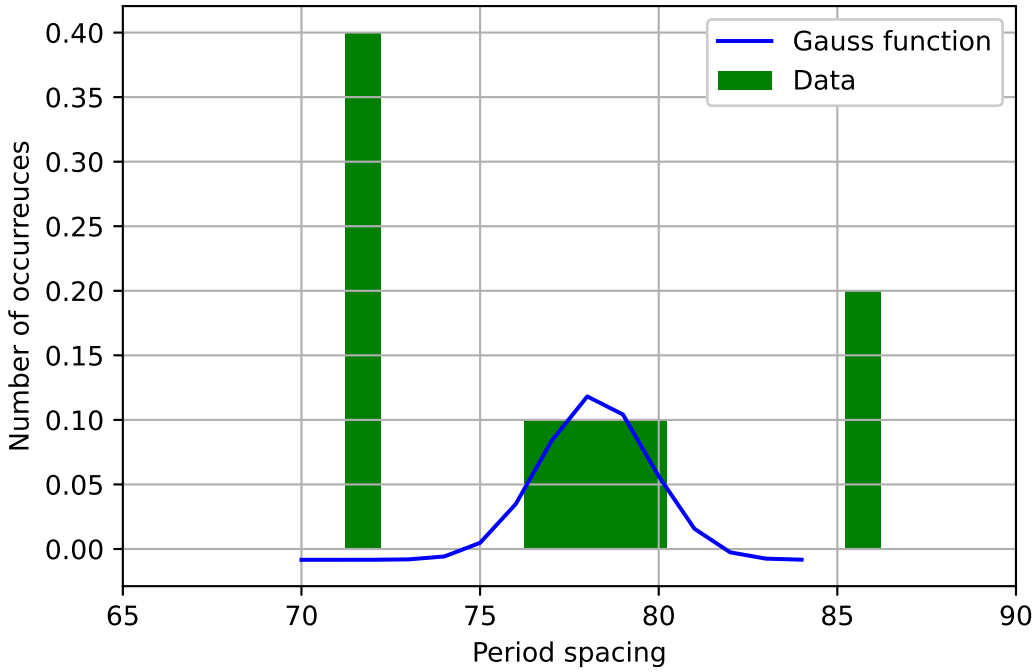

Rysunek 9: Histogram showing the distance distribution number for $l = 3$ with fitted Gaussian function in the range from 70 to 85 seconds, where the width of the bars is 3 seconds.

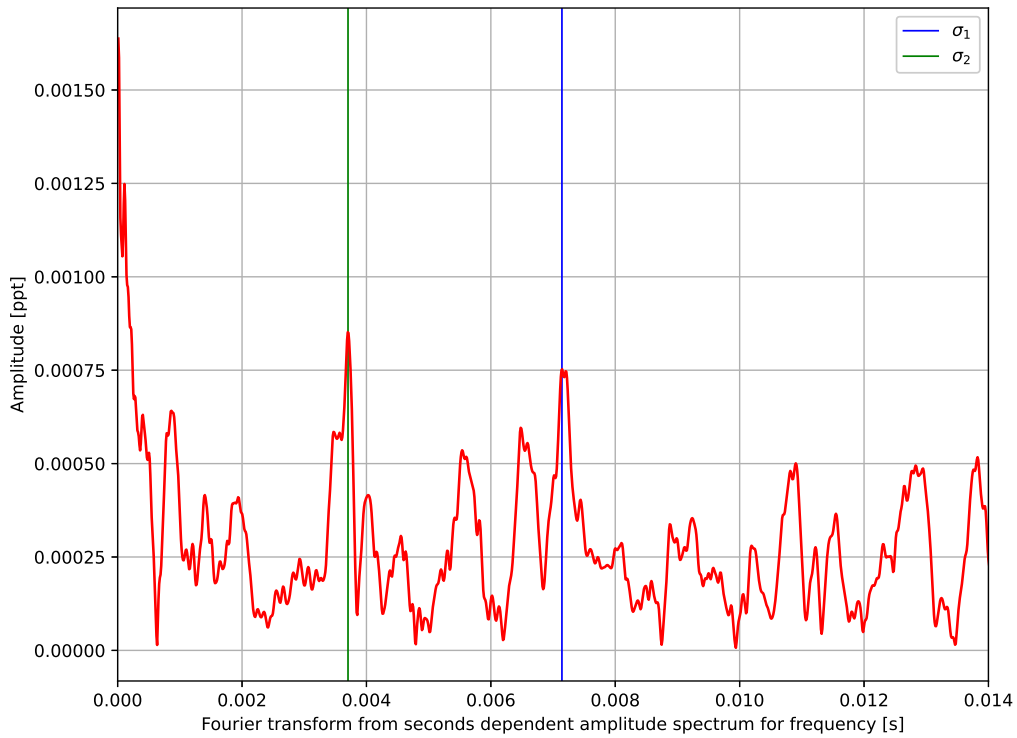

Rysunek 10: Fourier transform confirming the determination of Π with marked maxima of σ_1, σ_2 histograms for each identified signal.

Index	Frequency [s]	Period [s]	Amplitude [ppt]	Numbers l and m	Number n
0	11.687871	7392.278726	0.069794	2, -2	
1	11.691179	7390.186903	0.084929	2, -1	
2	11.692334	7389.456944	0.089297	2, 0	0
3	11.69395	7388.43609	0.061972	2, +1	
4	11.696643	7386.734885	0.051378	2, +2	
5	11.697566	7386.151938	0.042368	2	1
6	11.703568	7382.363789	0.045161	2	
7	12.139242	7117.412997	0.041216	2	3
8	12.141089	7116.330081	0.185183	2	4
9	12.143244	7115.067563	0.052738	2	5
10	12.145706	7113.625072	0.072152	2	6
11	12.616083	6848.401281	0.062762	2	7
12	12.620316	6846.104573	0.045573	2	8
13	12.621316	6845.561927	0.050248	2	9
14	12.623162	6844.56067	0.089982	2	10
15	12.624085	6844.060148	0.062989	2	11
16	12.62524	6843.434085	0.046195	2	12
17	12.626086	6842.975595	0.044561	2	13
18	13.134321	6578.185398	0.064605	2	14
19	13.136322	6577.183466	0.074395	2	15
20	13.138092	6576.29736	0.104344	2	16
21	13.141478	6574.603158	0.046138	2	17
22	13.655638	6327.057121	0.043131	3	
23	13.656946	6326.45094	0.07842	3	
24	13.658408	6325.773764	0.174031	3	
25	14.255286	6060.909523	0.052377	2	18
26	14.287989	6047.037274	0.091084	2	
27	14.290066	6046.158317	0.103591	2, -2	
28	14.921724	5790.215537	0.123525	2, -1	
29	14.923109	5789.678257	0.344852	2, 0	20
30	14.924495	5789.140705	0.100397	2, +1	
31	16.334549	5289.402252	0.076301	2, +2	
32	16.339859	5287.683324	0.056953	2	21
33	16.341013	5287.309928	0.051016	2	22
34	16.342012	5286.986562	0.042326	2	23
35	16.344091	5286.314043	0.041033	2	
36	17.187584	5026.884547	0.055428	2	
37	17.195433	5024.590059	0.065719	2	
38	17.196972	5024.140328	0.048017	2	
39	17.19828	5023.758093	0.038583	2	
40	17.199356	5023.443878	0.074763	2	
41	17.200357	5023.151426	0.116555	2, -2	
42	17.201973	5022.679678	0.244131	2, -1	
43	17.203358	5022.27539	0.660921	2, 0	30
44	17.204742	5021.87117	0.100748	2, +1	
45	17.205744	5021.578901	0.083403	2, +2	
46	17.206591	5021.331753	0.112716	2	31
47	17.208975	5020.636081	0.045892	2	32
48	17.209591	5020.456352	0.053044	2	33
49	17.211206	5019.985107	0.058084	2	34
50	17.212208	5019.693061	0.037217	2	35
51	17.218132	5017.965938	0.039706	2	36
52	17.685892	4885.249749	0.039499	1	0
53	17.691587	4883.677072	0.04821	1	
54	17.693665	4883.103766	0.044769	1	
55	17.69582	4882.509018	0.05444	1	
56	17.697973	4881.914939	0.076211	1	
57	17.699358	4881.532994	0.053501	1	
58	17.701668	4880.896028	0.065924	1	
59	17.703821	4880.302344	0.046614	1	
60	18.183971	4751.437299	0.047834	2	37

Index	Frequency [s]	Period [s]	Amplitude [ppt]	Numbers l and m	Number n
61	18.185587	4751.015204	0.040378	2	38
62	18.187281	4750.572758	0.065038	2, -2	
63	18.195129	4748.523528	0.069324	2, -1	
64	18.203054	4746.456169	0.672171	2 0	39
65	18.210979	4744.390613	0.067572	2, +1	
66	18.217905	4742.587021	0.052674	2, +2	
67	18.218828	4742.346711	0.043955	2	
68	18.246452	4735.167058	0.04267	1	8
69	20.232609	4270.334135	0.074524	1	
70	21.007235	4112.868817	0.040064	1	
71	21.008467	4112.627597	0.044996	1	
72	21.841496	3955.773082	0.117993	1	12
73	22.045019	3919.252663	0.043751	2	41
74	22.046482	3918.992592	0.201251	2	42
75	22.705687	3805.214158	0.048795	1	13
76	22.712612	3804.053864	0.040971	1	14
77	22.713535	3803.899253	0.048534	1	15
78	22.717461	3803.241982	0.039939	1	16
79	22.718384	3803.087438	0.087243	1, -1	
80	22.721462	3802.572169	0.509853	1, 0	17
81	22.724077	3802.134589	0.116377	1, +1	
82	23.616278	3658.493567	0.071092	1	
83	23.647057	3653.73169	0.046596	1	19
84	23.670372	3650.132747	0.043553	2	43
85	23.671988	3649.883639	0.045096	2	44
86	23.678913	3648.816124	0.046307	1	20
87	23.682299	3648.294502	0.052955	1	21
88	23.683069	3648.175799	0.048491	1	22
89	23.683992	3648.033599	0.061885	1	23
90	23.684839	3647.903162	0.061257	1	24
91	23.687763	3647.452874	0.042415	1	25
92	23.688686	3647.310731	0.040786	1	26
93	23.689301	3647.216171	0.062787	1	27
94	23.690918	3646.967167	0.064309	1	28
95	23.691763	3646.837101	0.087831	1, -1	
96	23.69969	3645.617326	0.996922	1, 0	29
97	23.707615	3644.398661	0.08374	1, +1	
98	23.708538	3644.256756	0.05529	1	30
99	23.709307	3644.138609	0.04838	1	31
100	23.710077	3644.020175	0.06274	1	32
101	23.711	3643.878301	0.047859	1	33
102	23.712231	3643.689249	0.049148	1	34
103	23.713078	3643.559121	0.043619	1	35
104	23.71454	3643.334353	0.061614	1	
105	23.715464	3643.192531	0.087175	1	
106	23.724773	3641.762916	0.044907	1	
107	23.729082	3641.101649	0.050071	1	
108	23.877359	3618.490579	0.048206	1	
109	24.706541	3497.049619	0.05248	1, -1	
110	24.710619	3496.472513	0.152824	1, 0	41
111	24.714005	3495.993534	0.048611	1, +1	
112	25.793957	3349.621805	0.047351	2	
113	25.802498	3348.513019	0.038077	2	46
114	25.804806	3348.213538	0.228419	2	47
115	26.95878	3204.892769	0.047304	1	
116	26.966476	3203.978102	0.04159	1	
117	31.044746	2783.079587	0.044616	2, -2	
118	31.070061	2780.812073	0.054514	2, -1	
119	31.073139	2780.536574	0.089261	2, 0	48
120	31.073986	2780.460796	0.06578	2, +1	

Index	Frequency [s]	Period [s]	Amplitude [ppt]	Numbers l and m	Number n
121	31.075064	2780.364372	0.073978	2, +2	
122	31.076372	2780.247308	0.493493	2	
123	31.077757	2780.123428	0.103449	2	
124	31.078833	2780.027198	0.057261	2	
125	31.079603	2779.958272	0.059969	2	
126	31.08045	2779.882525	0.069354	2	
127	31.081911	2779.751855	0.041901	2	
128	31.084297	2779.538476	0.060012	2	
129	31.092222	2778.830005	0.047492	2	
130	34.404331	2511.311715	0.038026	2	57